

Research Article

Entangled Polymer Surface Confinement, an Alternative Method to Control Stem Cell Differentiation in the Absence of Chemical Mediators

Chang C¹, Bherwani A², Simon M², Rafailovich M¹ and Jurukovski V^{1,*}

¹Department of Materials Science& Engineering, Stony Brook University, USA

²Department of Oral and Pathology, Stony Brook University, USA

³Department of Biology, Suffolk County Community College, USA

***Corresponding author:** Jurukovski V, Department of Materials Science & Engineering, Stony Brook University, 314 Engineering Bldg., Stony Brook, NY 11794-2275, USA

Received: July 15, 2014; **Accepted:** September 01,

2014; **Published:** September 24, 2014

Abstract

We have demonstrated that the moduli of spun cast and annealed polybutadiene films can be enhanced by nearly an order of magnitude, due to confinement near an attractive HF etched Si substrate interface. The region of enhancement scaled with the polymer radius of gyration and persisted for distances greater than twenty times the radius of gyration of the polymer, R_g , from the Si interface. We also showed that dental pulp stem cells (DPSC) can be plated directly on these films without any additional coatings and that the DPSCs were able to adjust their moduli in a continuous manner in response to that of the substrate. A critical value of the substrate modulus, $M_c = 2.3 \text{ MPa}$ was found which was independent of substrate molecular weight or thickness, such that for substrates with moduli $M > M_c$, the DPSC were induced to produce hydroxyapatite mineral deposits and upregulate gene expression of osteocalcin (OCN) and alkaline phosphatase (ALP), in the absence of any other soluble factors.

Keywords: Biominerization; Hydroxylapatite; Mechanical properties; Odontogenesis/Osteogenesis; Stem cells; Elastomers; Surface interactions

Abbreviations

PB: Polybutadiene; DPSC: Dental Pulp Stem Cells; SEM: Scanning Electron Microscopy; EDX: Energy-dispersive X-ray Spectroscopy; GIDX: Grazing Incidence X-ray Diffraction; RT-PCR: Real Time-Polymerase Chain Reaction; OCN: Osteocalcin; ALP: Alkaline Phosphatase; LSCM: Laser Scanning Confocal Microscopy; Dex: Dexamethasone; RMS: Root Mean Squared; AFM: Atomic Force Microscopy; SMFM: Shear Modulation Force Microscopy

Introduction

Recently, considerable advances have been made our understanding of the interaction between stem cells and materials scaffolds. In particular much effort has been expended on materials for the delivery of stem cells for regenerative medicine [1]. While the central focus is the healing of damaged tissues and organs, there is concern that the transplantation niche may not support cell proliferation or may promote unpredicted and undesired changes in cell differentiation. Numerous groups have experimented with hydrogels where the mechanical properties are controlled via the cross linking density. Even though these systems were able to demonstrate successfully that differentiation could be controlled via the substrate modulus, most of the gels required additional coatings to allow cell adhesion or mask the effect of excess cross linker which can segregate to the free surface [2,3]. In order to accomplish differentiation in the absence of any additional chemical factors or coatings, we propose an alternative method to cross linked hydrogel scaffolds. It has been previously established that confinement of long chain entangled polymers near an interactive surface, can pin the chains to the surface, forming an effective "strangulated" gel [4]. It was shown that

the influence of the confinement on the rheological properties of the films persisted for more than 10 polymer radii of gyration from the surface. Hence, through variation of the film thickness it was shown that the viscosity of the film can be changed by more than an order magnitude [5]. We therefore postulated that the mechanical response of the films can also be controlled simply by changing the film thickness of a polymer on a surface which interacted favorably with the polymer. Here we demonstrate that this is indeed the case when long chain, entangled elastomers are used. Furthermore, we show that this method can be used to determine the functional form, which, as expected, is continuous and differential, of the change in modulus with film thickness, or distance from the interacting surface. This system provides a convenient platform which allows us to ask several fundamental questions regarding stem cell response to changes in the substrate mechanics which cannot otherwise be addressed in a hydrogel system. First, since these polymers are hydrophobic, we must establish the ability of these substrates to promote cell adhesion in the absence of additional chemical factors or coatings. Second, assuming that the surfaces are adhesive, we can determine whether the cells adapt to changes in mechanics in a continuous manner, where even small differential changes can be measured. Finally, we can determine whether changes in the cell modulus induced by the surface can promote differentiation in the absence of additional soluble mediators.

Undifferentiated mesenchymal stem cells isolated from dental pulp (dental pulp stem cells-DPSCs) when grown in specific inducing media can differentiate and express markers of odontoblasts, osteoblasts, adipocytes or neuronal cells [6-10]. In addition, DPSCs have been shown to produce dentin when implanted in immuno-

compromised mice [6,8,11]. cDNA microarray analyses show that DPSCs have gene expression pattern similar to that of bone marrow mesenchymal stem cells [12]. Induction of DPSCs with dexamethasone (Dex), an active glucocorticoid analog, in presence of inorganic phosphate and ascorbic acid results in the production of a mineralized calcified matrix with sparsely distributed condensed nodules containing high levels of calcium [6]. DPSCs are located in the relatively soft environment of the pulp and differentiate into odontoblasts which produce mineralized matrix-dentin. Changes in the pulp as result of tooth damage or bacterial infection can trigger calcification of the pulp and effectively render the tooth dead. This transformation correlates with the influx of inflammatory cytokines and the change in the mechanical properties of the pulp [13,14]. Obviously changes in the chemical and physical properties of the environment induce signal transduction events leading to differentiation.

The use of materials whose mechanical properties can regulate or direct stem cell proliferation and differentiation offers exciting applications. Engler et al [2,3] used substrates made from polyacrylamide gels overlaid with collagen. In these experiments the mechanical properties were controlled by varying the acrylamide crosslinker and hence the cross-linking density. Although the mechanical properties of the collagen coating was not directly measured, cell differentiation was shown to correlate with the mechanical properties of the acrylamide gels obtained from bulk measurements, which were not sensitive to the actual moduli of the sample surface. In this model, the differences of moduli required to affect differentiation were large (1kPa- 100kPa), and may have been much larger than the surface deviations. In addition, both chemical and mechanical induction of differentiation was used.

In this paper, we introduce the use of polybutadiene (PB), which is a biocompatible, synthetic rubber material similar to the natural rubber gutta-percha, material used in dentistry to fill root canals. PB can be synthesized in the monodisperse form, with high molecular weight chains, ($M_w = 205K$, $M_w/M_n = 1.49$) such that $R_g = 135\text{\AA}$. Since PB is a rubber under ambient condition ($T_g = -95^\circ\text{C}$), the effect of surface interactions on PB films of varying thickness can be probed without the high temperature conditions described in the previous literature [4,5]. Furthermore, when annealed under these conditions, X-ray reflectivity in conjunction with atomic force microscopy, have shown that the films produced are extremely uniform with an RMS roughness less 6\AA [4]. Hence PB provides the ideal substrate for probing only the effects of variable substrate mechanics, without any chemical or topographical variations, on biological systems where the operational temperature range is restricted to 37°C . Here we describe the use of specially processed PB films whose surface properties and thickness can be characterized with nanometer precision, to produce substrates with controlled mechanical response, in order to investigate to what degree DPSC can sense the mechanics of the underlying substrates and determine whether a critical value exists for the modulus above which the cells will spontaneously differentiate.

Materials and Methods

Sample preparation

To prepare various thicknesses of PB spun-cast films, monodisperse PB ($M_w=205,800$, $M_w/M_n = 1.49$; Scientific Polymer

Products, Inc.) was dissolved in toluene (certified A.C.S.; ACROS) at different concentrations (w/v); 3, 5, 10, 20 and 25 mg/mL and then spun-cast at 2,500 rpm onto HF-etched wafers (Wafer World Corporation, West Palm Beach, FL) to produce of PB films with thicknesses of 200, 500, 1500, 2000 and 3000 \AA as measured by ellipsometry. PB films were then annealed in the ultra-high vacuum oven at 10^{-8} torr at 150°C for 24 h to remove the residual solvent and relax the polymer structure.

Cell isolation and culture

Dental pulp stem cells (DPSCs) strain AX3 were isolated from the third molar teeth (IRB #20076778) as previously described [11] and were grown in α -MEM media (Invitrogen) supplemented with 10% fetal bovine serum, 200 μM L-ascorbic acid 2-phosphate, 2 mM L-glutamine, 100 units/ml penicillin/ 100 $\mu\text{g}/\text{ml}$ streptomycin, and 10mM β -glycerophosphate. For chemical induction of osteogenesis/ odontogenesis, medium was supplemented with 10^{-8} M Dex (Sigma-Aldrich). The cells were grown at 37°C in 5% CO_2 .

Cell plating and proliferation

DPSCs were harvested, counted and then plated on tissue culture polystyrene plastics (TCP) and PB films at a density of 5,000 cells cm^2 . For the study of cell proliferation, the cell number was determined on day 3, 5 and 7 using a Hemacytometer (Hausser Scientific).

Shear modulation force microscopy (SMFM)

The moduli of PB films and DPSCs cultured on PB films were measured by atomic force microscopy (AFM, Dimension 3000; Digital Instruments, Santa Barbara, CA) using shear modulation force microscopy (SMFM). The experimental setup of the SMFM method was described in earlier articles [15,16]. Briefly, the AFM tip, applied to indent the surface, was laterally modulated and the mechanical response was fed into a lock-in amplifier and recorded. During the measurement, a normal indenting force of 25nN was exerted by the cantilever to maintain tip-surface contact, while a sinusoidal drive signal was applied to the piezo controlling the cantilever to induce a small oscillatory motion. The lateral deflection (response) amplitude of the cantilever was measured against the drive amplitude, both in mV, the response amplitude, therefore, being proportional to drive amplitude.

The moduli of films with different molecular weight were obtained using Bruker ICON AFM on the Peak Force QNM mode. Peak Force QNM (Quantitative NanoMechanics), an extension of Peak Force Tapping mode, enables quantitative measurement of nano-scale material properties such as modulus, adhesion, deformation and dissipation. Peak Force Tapping mode, the core technology behind Peak Force QNM performs a very fast force curve at pixel in the image. The peak interaction force of each of these force curves is then used as the imaging feedback signal. Peak Force Tapping mode modulates the Z-piezo at $\sim 2\text{kHz}$ with a default Peak Force Amplitude of 150 nm. Analysis of force curve data is done on the fly, providing a map of multiple mechanical properties (Adhesion, Modulus, Deformation, and Dissipation) that has the same resolution as the height image.

Nanoindentation

Instrumented indentation was performed using a nanoindenter (Micro Materials Nano Test) with diamond spherical indenters. Depth controlled indentations were performed with the maximum

depth set from 35 to 60 nm depending on the sample, and represented no more than 30% of the total film thickness. A 5 μ m radius of curvature conical indenter was used on the film samples, and a 200 μ m radius spherical indenter used on the bulk sample. Film substrates were mounted with an epoxy adhesive to aluminum sample holders for testing. Load-displacement data was obtained using a constant loading and unloading rate of 1 μ N/s. Typical maximum loads reached were on the order of 50-200 μ N. A 5 second hold segment was taken at the maximum displacement before unloading to take into account creep effects. On each sample, ten identical indentations were performed with a minimum spacing interval of 50 μ m between successive indents to ensure no interaction between residual plastic deformations. To determine elastic modulus of the films, the slope (S) of the initial unloading data in conjunction with the spherical contact area is used in the conventional Oliver and Pharr method [17].

Staining and laser scanning confocal microscopy (LSCM)

Immunocytochemistry was used to stain actin filaments and nuclei. Cells were washed with Ca, Mg-free phosphate buffered saline, pH 7.4 (PBS), fixed with 3.7% formaldehyde for 15 minutes, and permeabilized with 0.4% Triton X-100 in PBS. To visualize actin filaments the cells were incubated with 1:200 dilutions of Alexa Fluor 488 Phalloidin (Invitrogen, Carlsbad, CA). After 2 x 5 minute washes

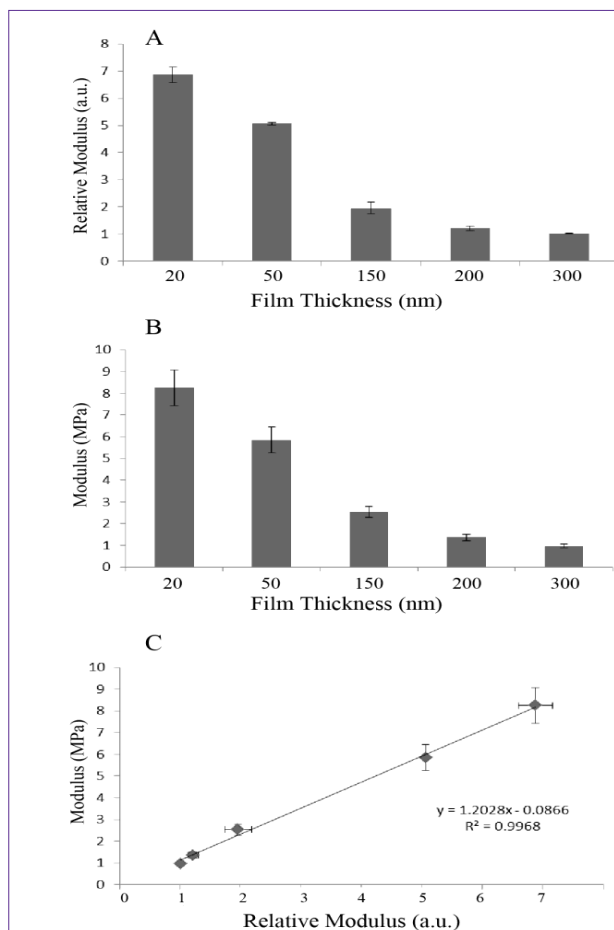


Figure 1: PB film thickness regulates its modulus. Moduli versus film thickness for PB (MW = 205K) as measured by SMFM (Panel A), and Hysitron nanoindentation (Panel B). The correlation between the methods is shown in Panel C.

in 0.05% Tween 20 in PBS propidium iodide (Sigma Chemical Co., St. Louis, CA) was added to visualize nuclei. Samples were analyzed and images captured using a Leica TCS SP2 LSCM (Leica micro-system Inc., Bannockburn, IL).

Scanning electron microscopy and energy dispersive X-ray (SEM/EDX)

Surface morphologies of PB films were characterized using scanning electron microscopy (SEM, LEO1550) at 20 kV acceleration voltage and 10 mm working distance. Samples were prepared by gently washing with deionized water to remove soluble salts from media and air-drying for 1 day. Samples were sputter-coated with gold for 15 seconds and loaded on aluminum stubs for SEM imaging. The elemental compositions of deposits on PB films were determined by using Energy Dispersive X-ray spectroscopy (EDX) in conjunction with SEM.

Real time-polymerase chain reaction

Total RNA was isolated using the RNeasy Mini kit (Qiagen, Valencia, CA) as described by the manufacturer. RNA concentrations were determined by absorbance at 260 nm; only samples with a ratio of OD 260:280>1.9 were used. For mRNA quantitation, 5 μ g of total RNA was separately reverse transcribed with 200 U Superscript II and 250 ng random primers (Invitrogen, Carlsbad, CA) as recommended by the manufacturer. Real-time PCR was performed in triplicate with 4 pmol amplifying primers and 8 μ l DNA in a final volume of 20 μ L using QuantiTect SYBR Green PCR Kit (Qiagen, Valencia, CA). Real-time PCR was carried out and analyzed using MJ Research Opticon System (MJ Research, Waltham, MA), a service provided by the DNA sequencing facility of Stony Brook University. The expression levels of bone alkaline phosphatase (ALP) and osteocalcin (OCN) were determined using gene specific primers (ALP- forward primer: 5'-GTACTGGCGAGACCAAGCGCAA-3' and reverse primer: 5'-ACCCCACACAGGTAGGCGGT-3'; OCN- forward primer: 5'-ATGAGAGGCCCTCACACTCCTCG-3' and reverse primer: 5'-GTCAGCCAACTCGTACAGTCC-3'). 18S served as control using forward primer: 5'-GTAACCCGTTGAACCCCATT-3' and reverse primer: 5'-CCATCCAATCGGTAGTAGCG -3'.

Results and Discussion

Control of thin film moduli via surface confinement

In Figure 1A we plot the relative moduli of the annealed PB (Mw=205K) films for different film thicknesses using the SMFM method where we can see that the moduli decrease with increasing film thickness. The same samples were also measured with a Hysitron nanoindenter (Figure 1B), and in Figure 1C we plot the SMFM vs the nanoindentation measurements where we find a linear relationship, indicating that the relative values between samples are similar, despite differences in the techniques. The accuracy of the slope,

Table 1: Characteristic properties of polybutadiene films produced with different Mw polymers.

Mw [Daltons]	56,000	205,000	400,000
Rg [nm]	7.1	13.5	18.9
Mo [MPa]	4.2	5.1	6.3
t ₀ [nm ⁻¹]	125	182	250
t' ₀	1.76	1.35	1.32

$m=1.20(5)$, allows us to calibrate the SMFM measurements relative to those obtained with the Hysitron calibrated nanoindenter, where we find that the moduli of the PB films, of $Mw=205K$, are in the range of 1-8 MPa for films ranging from 20nm-300 nm. It has previously been demonstrated by Li et al. [18] that the effective viscosity of a polymer film at a temperature above its glass transition, T_g , increases exponentially with decreasing film thickness. The phenomena was explained in terms of the formation of an adsorbed brushy state at the interface with the substrate, which in turn can trap other chains, not in contact with the surface, slowing down, but not stopping their ability to diffuse or flow in a manner similar to a "strangulated" gel, where, the thickness of this gel layer had been shown by Zheng et al [5] to scale with Rg , the radius of gyration of the polymer. In order to determine whether the decrease in modulus with thickness is correlated to the polymer structure, as opposed to the proximity of the hard Si interface, we also tested films of two other molecular weights, whose properties are listed in Table 1. In Figure 2A we plot the surface modulus, M , vs film thickness, t , for the film of three molecular weights, where the solid lines in each case are fits to an exponential function of the form;

$$\text{Equation 1: } M=M_0 \exp(-t/t_0)$$

Where M_0 is the highest value obtainable in the limit $t \rightarrow 0$ and t_0 is the half width for propagation of the surface modulus.

The fit parameters for each molecular weight are tabulated in Table 1 where we see that, as expected, the sample with the highest molecular weight, or the highest viscosity, also has the largest initial modulus and the longest decay constant. In Figure 2b we plot the moduli as a function of the thickness normalized by the polymer radius of gyration, also listed in Table 1, where the solid lines are fits to the function;

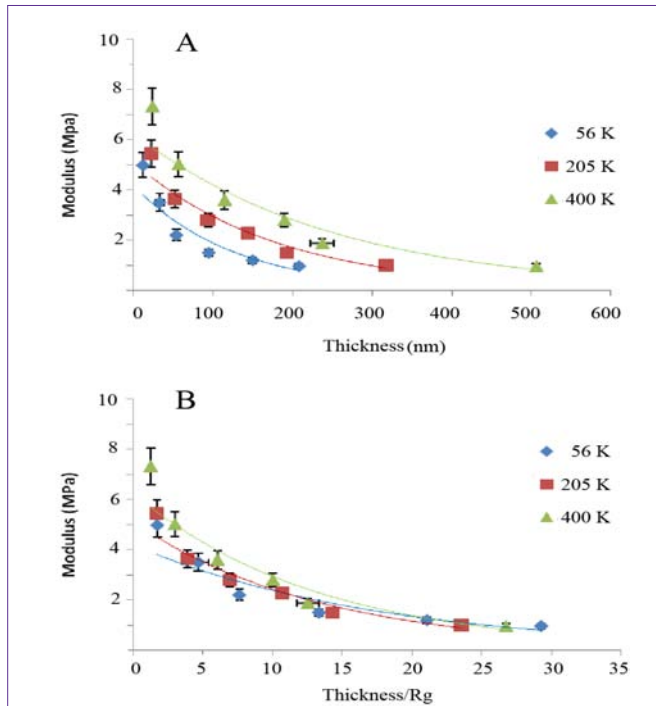


Figure 2: The moduli of spun cast PB films on HF etched Si substrates for three different molecular weights (A) as a function of film thickness and (B) film thickness scaled by the polymer radius of gyration, Rg .

$$\text{Equation 2: } M=M_0 \exp(t'/t'_0) \text{ where } t'=t/R_g$$

From the figure we now find that (a) the enhanced surface modulus of the films persists for more than 20 Rg or for similar distances to those reported previously by Zheng et al [5], for the diffusion coefficient and the film viscosity and (b) the decay constants of the three curves are now very similar, or related to each other by the scaling factor; $t'_0 \sim t_0 Rg$, confirming the role of the polymer chain structure in propagating the effect of interfacial surface confinement on the mechanical properties of the films. Hence, we can conclude that it is possible to produce thin films from PB where the surface moduli can be varied continuously in a differentially small manner, by nearly an order of magnitude simply by varying either the film thickness or the molecular weight, without any additional exogenous chemical factors.

The influence of substrate mechanics on cell proliferation and actin filament structure

We then evaluated PB for its ability to support DPSC proliferation. Cells were placed on PB films of $Mw=205K$ with two thicknesses, 23nm and 193nm, labeled "thin" and "thick" or corresponding to "hard" and "soft" substrates of moduli, $M=5.6\text{ MPa}$ and 1.5 MPa , respectively. The cells were counted at 3, 5 and 7 days after plating. As seen in Figure 3A, population doubling times on the thin PB substrate (50.1 ± 1.7 h) were 25% greater compared to cultures grown on TCP (41.5 ± 4.2 h, $p < 0.05$), whereas the population doubling time on the thick PB surface (76.5 ± 2.5 h) was increased by ~84% ($p < .005$). At day 7, replicate plates were stained with Alexa Fluor 488-Phalloidin to visualize actin filaments and propidium iodide to visualize cell nuclei. As seen in Figure 3B, actin filament organization was correlated to the substrate mechanics. On TCP and thin PB the actin fibers were well extended, whereas on thick PB the actin fibers were no longer aligned. Similar results were also reported by Ghosh et al. [19] who observed that fibroblasts plated on harder hyaluronic acid (HA) cross-linked hydrogel substrates had more extended actin filaments and exerted larger traction forces compared to cells plated on softer cross-linked

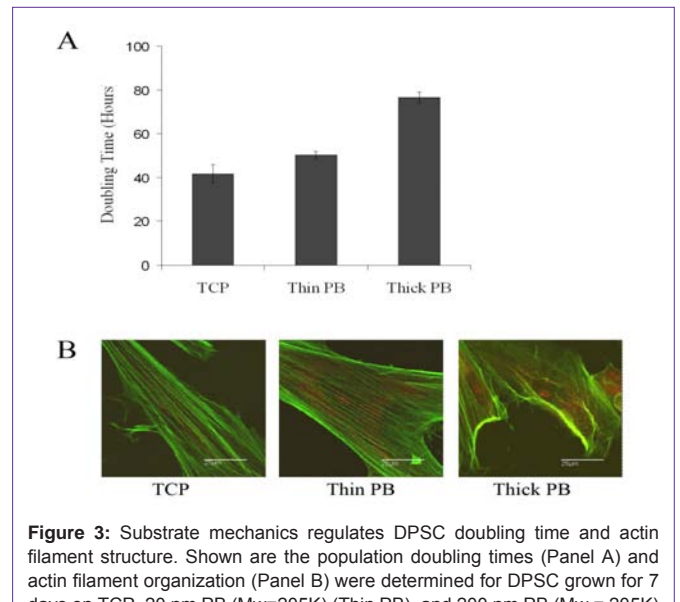


Figure 3: Substrate mechanics regulates DPSC doubling time and actin filament structure. Shown are the population doubling times (Panel A) and actin filament organization (Panel B) were determined for DPSC grown for 7 days on TCP, 20 nm PB ($Mw=205K$) (Thin PB), and 200 nm PB ($Mw = 205K$) (Thick PB).

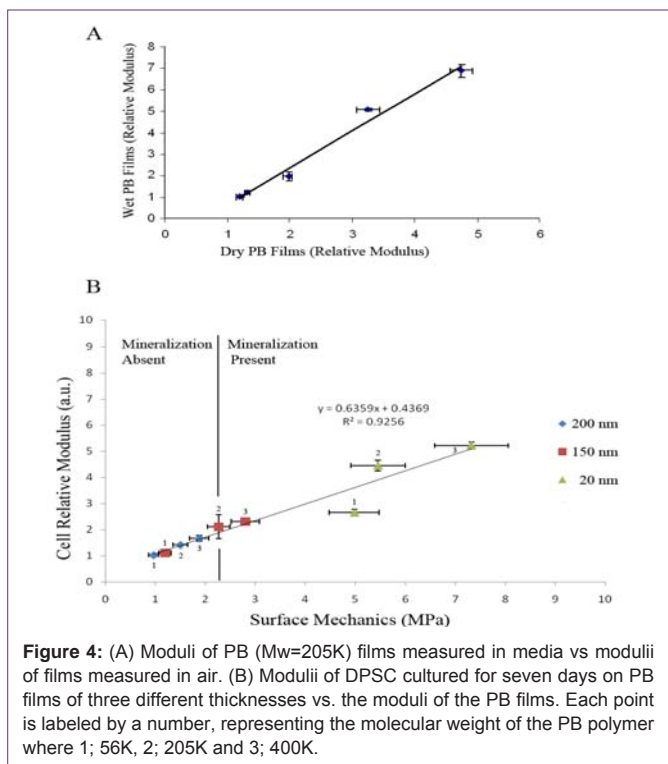


Figure 4: (A) Moduli of PB ($M_w=205K$) films measured in media vs moduli of films measured in air. (B) Moduli of DPSC cultured for seven days on PB films of three different thicknesses vs. the moduli of the PB films. Each point is labeled by a number, representing the molecular weight of the PB polymer where 1; 56K, 2; 205K and 3; 400K.

HA substrates. Since cell division is in part regulated by the ability of cells to exert large traction forces [19], the increased doubling time on the softer PB substrate may be due to the inability of the cells to exert adequate traction forces.

Correlating cell and substrate mechanical properties

The ability of the cells to sense the substrate mechanics was determined by simultaneously measuring the moduli of DPSC and the substrate on which they were plated. The results for measurements obtained seven days after plating are shown in Figure 4 [20]. In Figure 4A we plot the moduli of the substrate measured in media vs. the moduli measured in air, where we see a slope of unity, indicating that no hydration or softening of the PB surface occurred as a result of incubation. In the Figure 4B we plot the relative moduli of live DPSC vs. the surface modulus of the substrate for three different film thicknesses. From the figure we see that an excellent linear correlation is obtained, indicating that after one week incubation the cells can track even small differences in the modulus of the underlying substrate. Furthermore, from the figure we can clearly see that both the cell moduli, as well as the substrate moduli are primarily a function of the PB molecular weight, rather than the film thickness. Hence the moduli of the cells as well as those of the underlying films depend on the details of the polymer chain structure and their interaction with the Si substrates.

Mechanotransduction

The cells were further incubated for 21 days on soft (200 nm, $M_w=205K$) hard (20 nm, $M_w=205K$) substrates in order to determine whether the substrate mechanics alone would induce differentiation in the absence of other soluble factors. As a positive control a set was also cultured on the same substrates with added dexamethasone, a factor known to induce DPSC to differentiate along osteogenic

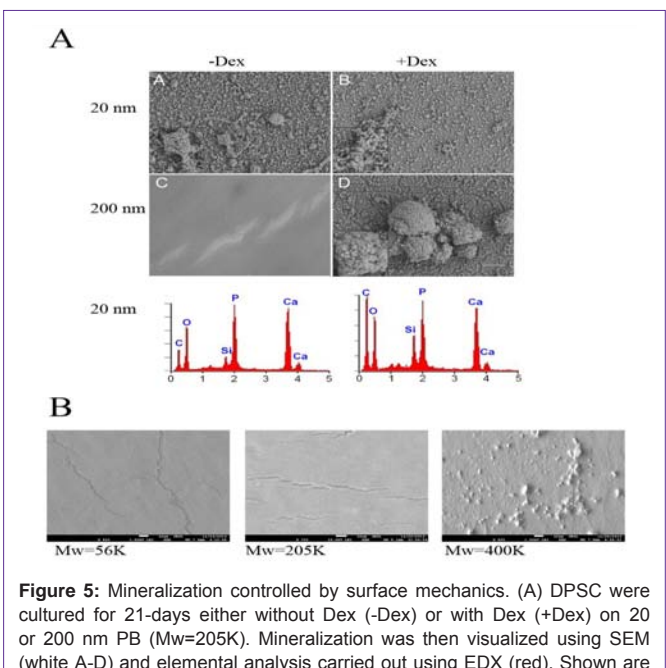


Figure 5: Mineralization controlled by surface mechanics. (A) DPSC were cultured for 21-days either without Dex (-Dex) or with Dex (+Dex) on 20 or 200 nm PB ($M_w=205K$). Mineralization was then visualized using SEM (white A-D) and elemental analysis carried out using EDX (red). Shown are the results for the 20 nm PB samples; identical results for the +Dex were obtained for the 200 nm samples; no mineralization was seen without Dex on the 200 nm samples. (B) DPSC were cultured for 21 days on 150 nm PB films $M_w=56K$ (G), $M_w=205K$ (H), and $M_w=400K$ (I) and SEM carried out to visualize mineralization. The properties of the 150 nm PB surfaces are given in Tables 1 and 2.

lineage. After 21 days, the substrates were dried and examined with SEM and EDX in order to determine whether mineralized deposits were present. The results are shown in Figure 5A. From the figure we can see that the cells treated with dexamethasone produced copious mineral deposits, on both thick and thin substrates, regardless of the modulus of the substrate. EDX analysis, shown in the lower panel, indicates that the deposits are composed of hydroxyapatite. SEM images of the DPSC incubated without addition of dexamethasone show no mineral deposition on the thick (soft) PB substrate, while a very large amount of deposits, which EDX confirms as hydroxyapatite, is seen on the thin (hard) substrate, indicating that mechanotransduction had occurred. DPSCs were also incubated on PB films of the three thicknesses and three molecular weights shown in Figure 4 without dexamethasone. The results consistently showed that regardless of thickness or molecular weight, no biomineratization occurred on films whose moduli were smaller than a critical value of 2.3 MPa, (marked by the solid line), while large amounts of mineral deposits were observed on substrates whose moduli were higher than this value. An interesting case, which clearly illustrates the importance of the modulus, is observed for the 150 nm thick films. From Figure 4 we see that the moduli of films of this thickness from PB of $M_w=400K$ have moduli greater than the critical value, while films of $M_w=56K$ and 205K have moduli less than this value. In Figure 5B we show the SEM images of these films following a 21 day incubation by the

Table 2: Biomineratization for 150 nm thick films.

Mw [Daltons]	56,000	205,000	400,000
Thickness [nm]	150	150	150
Thickness/Rg	21.1	11.1	7.9
Biomineratization (no Dex)	No	No	Yes

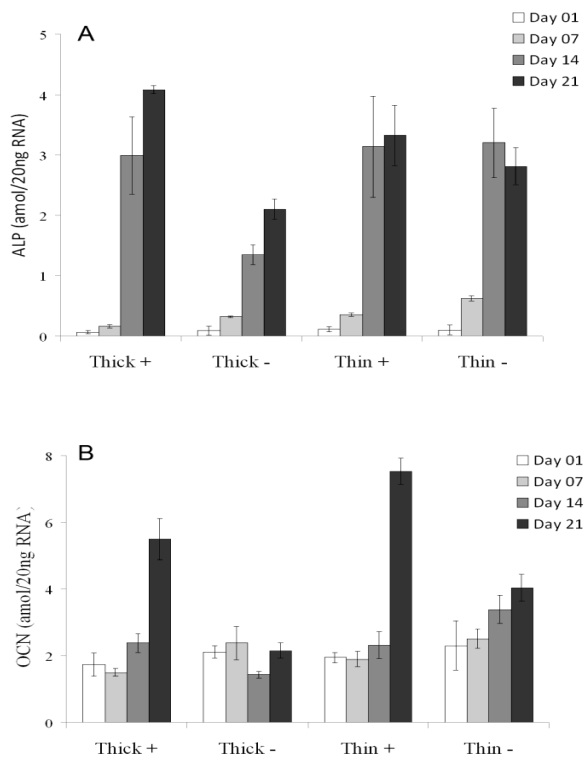


Figure 6: DPSC were grown on 20 nm PB (thin; Mw = 205K) or 200 nm PB (thick; Mw = 205K) in the presence (+) or absence (-) of dexamethasone. ALP (Panel A) and OCN (Panel B) gene expression were measured by RT-PCR at day 1, 7, 14, and 21 post-plating cells with levels normalized to 18S RNA.

DPSC, where we see that biominerization occurred only on the Mw=400K films, indicating that mechanotransduction, rather than film thickness was the primary factor in triggering differentiation.

Cell differentiation

DPSC differentiation was monitored as a function of alkaline phosphatase (ALP) and osteocalcin (OCN) mRNA expression both of which are up-regulated during odontogenesis and osteogenesis. Shown in Figure 6 are the expression levels in cells cultured on PB (Mw=205K) film of thickness, 20 nm (thin) and 200 nm (thick) for 7, 14, and 21 days in the presence or absence of Dex. As can be seen in Panel A, ALP expression increased in all samples by day 7, with larger increases observed by day 14. Comparable increases were observed in cultures grown on thick PB with dexamethasone or on thin PB with or without dexamethasone. This increase was nearly twice as large as that in cells grown on thicker PB substrate without dexamethasone. The expression of OCN shown in Panel B was also enhanced by growth with dexamethasone and was 3-fold greater at 21 days post-treatment compared to day 1. Again, in the absence of dexamethasone cultures grown on thin and thick PB differed. Those on thin PB showed 1.6-fold increase in OCN expression, whereas those on thick PB showed no increase. Thus, both ALP and OCN levels followed increases in cell moduli and biominerization supporting the notion that these processes may be coordinately regulated by substrate mechanics, as well as, by soluble differentiation inducers (e.g., Dex).

Conclusion

We have demonstrated that the moduli of polybutadiene films

spun cast and annealed on HF etched Si substrates are significantly enhanced over the bulk values due to confinement by the Si substrate. The region of enhancement scales with the polymer radius of gyration and persists for distances greater than Rg from the Si interface. DPSCs plated on these films are able to adjust their moduli in a continuous manner in response to that of the substrate. A critical value of the substrate modulus, $M = 2.3 \text{ MPa}$ was found which was independent of substrate molecular weight or thickness. Mechanotransduction, which resulted in the production of hydroxyapatite mineral deposits in the absence of any other soluble factors, was observed for DPSCs plated on substrates whose moduli were higher than this value.

Acknowledgement

This work was supported in part by the NSF-Inspire program, award number; DMR 1344267.

References

1. Mimeaule M, Hauke R, Batra SK. Stem cells: a revolution in therapeutics-recent advances in stem cell biology and their therapeutic applications in regenerative medicine and cancer therapies. *Clin Pharmacol Ther.* 2007; 82: 252-264.
2. Engler AJ, Sen S, Sweeney HL, Discher DE. Matrix elasticity directs stem cell lineage specification. *Cell.* 2006; 126: 677-689.
3. Tse JR, Engler AJ. Stiffness gradients mimicking in vivo tissue variation regulate mesenchymal stem cell fate. *PLoS One.* 2011; 6: e15978.
4. Zhao W, Rafailovich MH, Sokolov J, Fetter L, Plano R, Sanyal MK, et al. Wetting properties of thin liquid polyethylene propylene films. *Phys Rev Lett.* 1993; 70: 1453-1456.
5. Zheng X, Rafailovich M, Sokolov J, Strzheemechny Y, Schwarz SA, Sauer BB, et al. Long-range effects on polymer diffusion induced by a bounding interface. *Physical Review Letters.* 1997; 79: 241-244.
6. Gronthos S, Mankani M, Brahim J, Robey PG, Shi S. Postnatal human dental pulp stem cells (DPSCs) in vitro and in vivo. *Proc Natl Acad Sci U S A.* 2000; 97: 13625-13630.
7. Almushayt A, Narayanan K, Zaki AE, George A. Dentin matrix protein 1 induces cytodifferentiation of dental pulp stem cells into odontoblasts. *Gene Ther.* 2006; 13: 611-620.
8. Gronthos S, Brahim J, Li W, Fisher LW, Cherman N, Boyde A, et al. Stem cell properties of human dental pulp stem cells. *J Dent Res.* 2002; 81: 531-535.
9. Miura M, Gronthos S, Zhao M, Lu B, Fisher LW, Robey PG, et al. SHED: stem cells from human exfoliated deciduous teeth. *Proc Natl Acad Sci U S A.* 2003; 100: 5807-5812.
10. Nosrat IV, Smith CA, Mullally P, Olson L, Nosrat CA. Dental pulp stem cells provide neurotrophic support for dopaminergic neurons and differentiate into neurons in vitro; implications for tissue engineering and repair in the nervous system. *European Journal of Neuroscience.* 2004; 19: 2388-2398.
11. Batouli S, Miura M, Brahim J, Tsutsui TW, Fisher LW, Gronthos S, et al. Comparison of stem-cell-mediated osteogenesis and dentinogenesis. *J Dent Res.* 2003; 82: 976-981.
12. Shi S, Robey PG, Gronthos S. Comparison of human dental pulp and bone marrow stromal stem cells by cDNA microarray analysis. *Bone.* 2001; 29: 532-539.
13. Cooper PR, Takahashi Y, Graham LW, Simon S, Imazato S, Smith AJ, et al. Inflammation-regeneration interplay in the dentine-pulp complex. *J Dent.* 2010; 38: 687-697.
14. Goldberg M, Farges JC, Lacerda-Pinheiro S, Six N, Jegat N, Decup F. Inflammatory and immunological aspects of dental pulp repair. *Pharmacol Res.* 2008; 58: 137-147.
15. Ge S, Pu Y, Zhang W, Rafailovich M, Sokolov J. Shear modulation force microscopy study of near surface glass transition temperatures. *Physical Review Letters.* 2000; 85: 2340-2343.

16. Pu Y, Ge S, Rafailovich M, Sokolov J, Duan Y, Pearce E, et al. Surface transitions by shear modulation force microscopy. *Langmuir*. 2001; 17: 5865-5871.
17. Oliver WC, Pharr GM. An improved technique for determining hardness and elastic modulus using load and displacement sensing indentation experiments. *J. Materials Res.* 1992; 7: 1564-1583.
18. Li C, Koga T, Li C, Jiang J, Sharma S, Narayanan S, et al. Viscosity measurements of very thin polymer films. *Macromolecules*. 2005; 38: 5144-5151.
19. Ghosh K, Pan Z, Guan E, Ge S, Liu Y, Nakamura T. Cell adaptation to a physiologically relevant ECM mimic with different viscoelastic properties. *Biomaterials*. 2007; 28: 671-679.
20. Overney RM, Leta DP, Pictroski CF, Rafailovich M, Liu Y, Quinn J, et al. Compliance measurements of confined polystyrene solutions by atomic force microscopy. *Phys Rev Lett.* 1996; 76: 1272-1275.